

Static and dynamic stability of cracked multi-storey steel frames

Mustafa Sabuncu¹, Hasan Ozturk*¹ and Ahmed Yashar²

¹Department of Mechanical Engineering, Dokuz Eylul University, Tinaztepe, Buca, Izmir, Turkey

²The Graduate School of Natural and Applied Sciences, Dokuz Eylul University, Tinaztepe, Buca, Izmir, Turkey

(Received April 2, 2015, Revised January 13, 2016, Accepted February 13, 2016)

Abstract. Multi-storey frame structures are frequently exposed to static and dynamic forces. Therefore analyses of static (buckling) and dynamic stability come into prominence for these structures. In this study, the effects of number of storey, static and dynamic load parameters, crack depth and crack location on the in-plane static and dynamic stability of cracked multi-storey frame structures subjected to periodic loading have been investigated numerically by using the Finite Element Method. A crack element based on the Euler beam theory is developed by using the principles of fracture mechanics. The equation of motion for the cracked multi-storey frame subjected to periodic loading is achieved by Lagrange's equation. The results obtained from the stability analysis are presented in three dimensional graphs and tables.

Keywords: dynamic stability; storey frame; crack; buckling; finite element

1. Introduction

Multi-storey frames have been widely used in industrial buildings, bridges, gas or steam turbine blade packets, power plants and many mechanical engineering applications. These structures are exposed to static and dynamic loads depending on their operation conditions. Hereby, buckling and dynamic stability problems become important for multi-storey frame structures. In these frames, cracks may initiate due to earthquakes, accidents, corrosion or fatigue and grow up. As the crack affects the static and dynamic behaviors of a structure, so the buckling load and dynamic stability regions of these structure changes. In recent years, the static and dynamic stabilities of frame structures have been investigated by various methods.

The finite element approach has been used to determine the regions of dynamic stability of beams and framed structures by Brisseghella *et al.* (1998). Xu and Liu (2002) have presented a practical method for the stability analysis of semi-braced steel frames with the effect of semi-rigid behaviour of beam-to-column connections being taken into account. Ozmen and Girgin (2005) have developed a practical method based on computing an approximate value for determining the buckling loads of multi-storey frames. Girgin and Girgin (2006) have proposed a generalized numerical method to derive the static and dynamic stiffness matrices and to handle the nodal load

*Corresponding author, Associate Professor, E-mail: hasan.ozturk@deu.edu.tr

vector for static analysis of non-uniform Timoshenko beam-columns under several effects. Their method is applicable to some stability problems. An approach for evaluating the elastic buckling loads for multi-storey unbraced steel frames subjected to variable loading or non-proportional loading has been affirmed by Xu and Wang (2007). Choi and Yoo (2009) have proposed a method to overcome the weaknesses inherent in traditional elastic buckling analysis, based on the system buckling approach for the design of multi-story frames. Sakar *et al.* (2012) have studied the in-plane dynamic stability of multi-span frames, which are composed of columns and beams subjected to periodic loading using the Finite Element Method. Caddemi and Caliò (2013) have derived the exact stability stiffness matrix of an Euler-Bernoulli column in presence of an arbitrary number of concentrated cracks. Concentrated cracks are modelled as Dirac's delta singularities superimposed to a uniform flexural stiffness. In their study, the exact evaluation of the buckling loads and the corresponding buckling modes, consistent with the distributed parameter model, have been obtained through the application of the Wittrick-Williams algorithm. Buckling analysis has been examined for one-bay multi-cracked frames. Xu and Zhuang (2014) have investigated the elastic stability of unbraced steel frames subjected to a non-uniform elevated temperature distribution based on the concept of storey based buckling.

Buildings, bridges, turbines, power line towers etc. are subjected to numerous dynamic excitations such as wind, moving loads, earthquakes, hydrodynamic forces and pulsating loads produced by rotating machinery etc. These external disturbances could affect the vibration behaviour of structures especially when they combine with static preload. For certain values of exciting frequencies an entirely different type of resonance will occur and the structure is said to be dynamically unstable. Therefore the buckling and dynamic stability analyses are very important for these structures (Ozturk *et al.* 2016). Furthermore, although not in a large number, a number of studies are reported in literature dealing with the static and dynamic stability of cracked multi-storey steel frames. Mohammed (2001) has examined the effect of loss of support on behavior of multi-storey cracked frames subjected to vertical and horizontal loads taking into consideration the soil-structure interaction effect by using the photoelastic and Finite Element methods. Ibrahim *et al.* (2013) have investigated the effects of crack depth and crack location on the in-plane free vibration cracked frame structures numerically by using the Finite Element Method. The natural frequency analysis of beams with multiple cracks and multi-bay & storey frames with cracked beams has been studied by Labib *et al.* (2014). In this study, the natural frequencies are obtained using a new method in which a rotational spring model is used to represent the cracks.

As seen in the above literature review, in-plane dynamic stability analysis of cracked multi-storey frames, which are composed of columns and beams and subjected to periodic loading, has not been studied prior to this paper. There is one similar study (Ozturk *et al.* 2016) belonging to the authors in literature and this study (Ozturk *et al.* 2016) is concerned with dynamic stability analysis of multi-bay frame structures. In this paper, the effects of number of storey, static and dynamic load parameters, crack depth and crack location on static and dynamic stability of cracked multi-storey frame structures subjected to periodic loading have been investigated numerically by using the Finite Element Method. A crack element based on the Euler beam theory is developed by using the principles of fracture mechanics. Periodic loading is considered to be applied to each column member belonging the top storey as an axial load and no loading is applied on the beams. Using energy expressions in conjunction with Bolotin's approach, the study is carried out employing various disturbing frequency ranges in which the multi-storey cracked frame is to be unstable.

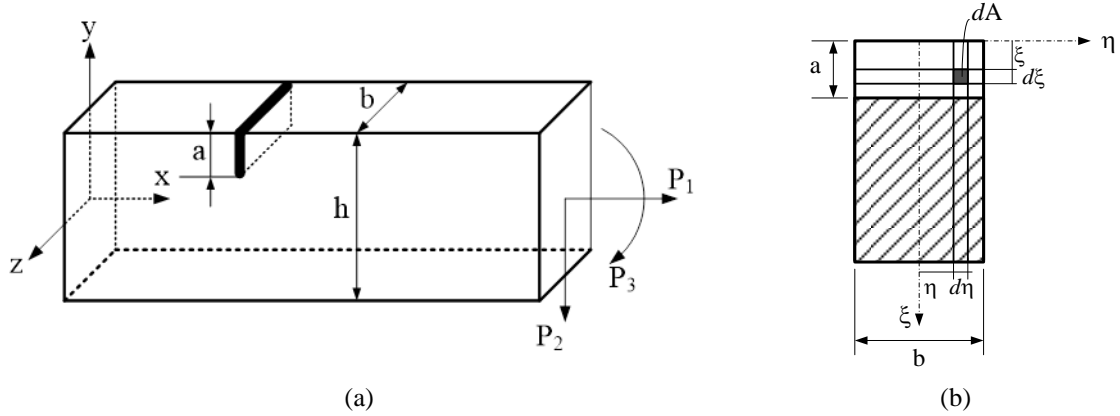


Fig. 1 (a) Schematic view of a cracked beam under generalized loading conditions, (b) geometry of cracked section showing integral limits

2. The cracked beam element theory

The additional strain energy due to the existence of a crack can be expressed as (Karaagac *et al.* 2009, Zheng and Kessissoglou 2004)

$$\Pi_c = \int_{A_c} G dA \quad (1)$$

where G is the strain energy release rate function and A_c is the effective cracked area. The strain energy release rate function G can be expressed as (Zheng and Kessissoglou 2004)

$$G = \frac{1}{E} \left[(K_{I1} + K_{I2} + K_{I3})^2 + K_{II1}^2 \right] \quad (2)$$

K_{In} and K_{IIn} ($n=1,2,3$) are the stress intensity factors of the two modes of fracture (opening and sliding types) corresponding to generalized loading P_n , respectively. The stress intensity factor K_{I2} is ignored (Ibrahim *et al.* 2013).

$$K_{I1} = \frac{P_1}{bh} \sqrt{\pi\xi} F1\left(\frac{\xi}{h}\right), K_{I3} = \frac{6P_3}{bh^2} \sqrt{\pi\xi} F2\left(\frac{\xi}{h}\right), K_{II2} = \frac{P_2}{bh} \sqrt{\pi\xi} F3\left(\frac{\xi}{h}\right) \quad (3)$$

where, a generalized loading is indicated by three general forces: an axial force P_1 , shear force P_2 and bending moment P_3 as seen in Fig. 1(a) and the correction functions $F1$, $F2$ and $F3$ are given in Appendix.

The elements of the overall additional flexibility matrix c_{ij} can be expressed as (Ibrahim *et al.* 2013)

$$c_{ij} = \frac{\partial \delta_i}{\partial P_i} = \frac{\partial^2 \Pi_c}{\partial P_i \partial P_j} \quad (i, j = 1, 2, 3 \dots) \quad (4)$$

Substituting Eqs. (1)-(3) into Eq. (4) yields the general equation for the local compliances as

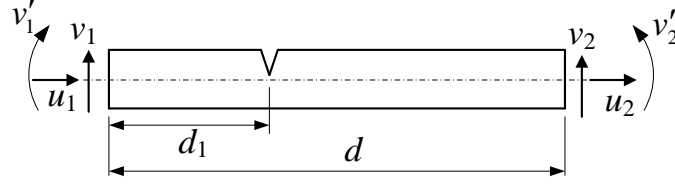


Fig. 2 Crack element model

follows (considering that all K 's are independent from η ; η : see Fig. 1(b))

$$c_{ij} = \frac{b}{E'} \frac{\partial^2}{\partial P_i \partial P_j} \int_0^a \left\{ \left[\frac{P_1}{bh} \sqrt{\pi\xi} F1\left(\frac{\xi}{h}\right) + \frac{6P_3}{bh^2} \sqrt{\pi\xi} F2\left(\frac{\xi}{h}\right) \right]^2 + \frac{P_2^2}{b^2 h^2} \pi\xi F3^2\left(\frac{\xi}{h}\right) \right\} d\xi \quad (5)$$

($i, j = 1, 2, 3, \dots$)

where c_{ij} is the local flexibility matrix.

The crack produces a local additional displacement between the right and left sections of the crack in a similar way as an equivalent spring. The spring effects are introduced to the system by using the local flexibility matrix given by Eq. (5). Multi-storey frame is modeled by using the Finite Element Method. The beam that forms the frame is assumed to be an Euler beam. The beam element has 2 nodes with three degrees of freedom in each node. The element is considered to be split into two segments by the crack as shown in Fig. 2. The cracked element has 2 nodes with three degrees of freedom in each node. They are denoted as lateral bending displacements (v_1, v_2), slopes (v_1', v_2'), and longitudinal displacements (u_1, u_2).

The displacements for the left and right parts of the cracked element and FEM's are described in detail in Ref. (Ibrahim *et al.* 2013). The generalized displacement vector with respect to local reference coordinates can be expressed as

$$q = [u_1 \quad v_1 \quad v_1' \quad u_2 \quad v_2 \quad v_2'] \quad (6)$$

The relation between the local and global reference coordinates can be written as

$$q = T\bar{q} \quad (7)$$

where T is the transformation matrix.

$$T = \begin{bmatrix} \cos\theta & \sin\theta & 0 & 0 & 0 & 0 \\ -\sin\theta & \cos\theta & 0 & 0 & 0 & 0 \\ 0 & 0 & 1 & 0 & 0 & 0 \\ 0 & 0 & 0 & \cos\theta & \sin\theta & 0 \\ 0 & 0 & 0 & -\sin\theta & \cos\theta & 0 \\ 0 & 0 & 0 & 0 & 0 & 1 \end{bmatrix} \quad (8)$$

where θ is an angle between local and global reference coordinates.

3. Energy equations, the equation of motion and stability theory

Energy equations should be expressed separately from the crack element and intact elements on the left side of the crack element.

The elastic potential energy U :

For intact elements on the left side of the cracked element

$$U_L = \frac{1}{2} \left(\int_0^d EI(v_1'')^2 dx \right) + \frac{1}{2} \left(\int_0^d EA(u_1')^2 dx \right) \quad (9)$$

For the cracked element

$$U_C = \frac{1}{2} \left(\int_0^{d_1} EI(v_1'')^2 dx \right) + \frac{1}{2} \left(\int_0^{d_1} EA(u_1')^2 dx \right) + \frac{1}{2} \left(\int_{d_1}^d EI(v_2'')^2 dx \right) + \frac{1}{2} \left(\int_{d_1}^d EA(u_2')^2 dx \right) \quad (10)$$

For intact element on the right side of the cracked element

$$U_R = \frac{1}{2} \left(\int_0^d EI(v_2'')^2 dx \right) + \frac{1}{2} \left(\int_0^d EA(u_2')^2 dx \right) \quad (11)$$

Similarly, the kinetic energy T of an element of length d in an Euler beam is given as follows for the intact elements on the left side of the cracked element

$$T_L = \frac{1}{2} \left[\int_0^d \rho A(\dot{v}_1^2 + \dot{u}_1^2) dx \right] \quad (12)$$

For the cracked element

$$T_C = \frac{1}{2} \left[\int_0^{d_1} \rho A(\dot{v}_1^2 + \dot{u}_1^2) dx \right] + \frac{1}{2} \left[\int_{d_1}^d \rho A(\dot{v}_2^2 + \dot{u}_2^2) dx \right] \quad (13)$$

For intact element on the right side of the cracked element

$$T_R = \frac{1}{2} \left[\int_0^d \rho A(\dot{v}_2^2 + \dot{u}_2^2) dx \right] \quad (14)$$

V denote the work done by the axial force $P(t)$:

For intact elements on the left side of the cracked element

$$V_L = \frac{1}{2} P(t) \int_0^d (v_1')^2 dx \quad (15)$$

For the cracked element

$$V_C = \frac{1}{2} P(t) \int_0^{d_1} (v_1')^2 dx + \frac{1}{2} P(t) \int_{d_1}^d (v_2')^2 dx \quad (16)$$

For intact element on the right side of the cracked element

$$V_R = \frac{1}{2} P(t) \int_0^d (v_2')^2 dx \quad (17)$$

In order to obtain the equation of motion for the cracked multi-storey frame subjected to periodic loading shown in Fig. 3, lateral bending displacements (v_1, v_2), slopes (v_1', v_2'), and longitudinal displacements (u_1, u_2) Ref. (Ibrahim *et al.* 2013) are substituted into the energy Eqs. (9)-(15). Then, the elastic stiffness matrix $[k_e]$, mass matrix $[m_e]$ and geometric matrix $[k_{ge}]$ are obtained for both cracked finite element and intact finite elements. Mass and stiffness matrices of each beam element are used to form global mass and stiffness matrices. The dynamic response of a beam for a conservative system can be formulated by means of Lagranges equation of motion in which the external forces are expressed in terms of time-dependent potentials and then performing the required operations, the entire system leads to the governing matrix equation of motion

$$[M_e] \{\ddot{\bar{q}}\} + \left[[K_e] - P(t) [K_{ge}] \right] \{\bar{q}\} = 0 \quad (18)$$

where $[m_e]$, $[k_e]$ and $[k_{ge}]$ represent global mass matrices, elastic stiffness and geometric matrix, respectively.

As seen in Fig. 3, the periodic load $P(t) = P_0 + P_t \cos \Omega t$ with Ω equal to the existing frequency, which is considered to apply to each column member as an axial load. P_0 and P_t represent static and dynamic loads, respectively. There are no axial periodic forces on the beams. The static and time dependent components of the load can be represented as a fraction of the fundamental static buckling load P_{cr} . Therefore, substituting $P(t) = \alpha P_{cr} + \beta P_{cr} \cos \Omega t$ in Eq. (18) gives (Sakar *et al.* 2012)

$$[M_e] \{\ddot{\bar{q}}\} + \left[[K_e] - (\alpha P_{cr} + \beta P_{cr} \cos \Omega t) [K_{ge}] \right] \{\bar{q}\} = 0 \quad (19)$$

where, static load parameter is $\alpha = P_0/P_{cr}$ and dynamic load parameter is $\beta = P_t/P_{cr}$.

Eq. (19) denotes a system of second order differential equation with periodic coefficients of the Mathieu-Hill type. From the theory of linear equations with periodic coefficients, the boundaries between stable and unstable solutions of Eq. (19) are formed by periodic solutions of period T and $2T$, where $T = 2\pi/\Omega$. Bolotin (1967) has shown that the solutions with period $2T$ are of greater practical importance, as the widths of these unstable regions are usually larger than those corresponding to the solutions with period T . As a first approximation, assume a periodic solution with period $2T$. Using this solution along with Eq. (19) yields the following (Sakar *et al.* 2012)

$$\left[[K_e] - \left(\alpha + \frac{1}{2} \beta \right) P_{cr} [K_{ge}] - \frac{\Omega^2}{4} [M_e] \right] \{\bar{q}\} = 0 \quad (20)$$

This equation represents the solution of three related problems:

- i. Free vibration with $\alpha=0, \beta=0$ and $\omega=\Omega/2$ the natural frequency.

$$\left[[K_e] - \omega^2 [M_e] \right] \{\bar{q}\} = 0 \quad (21)$$

- ii. Static stability with $\alpha=1, \beta=0$ and $\Omega=0$.

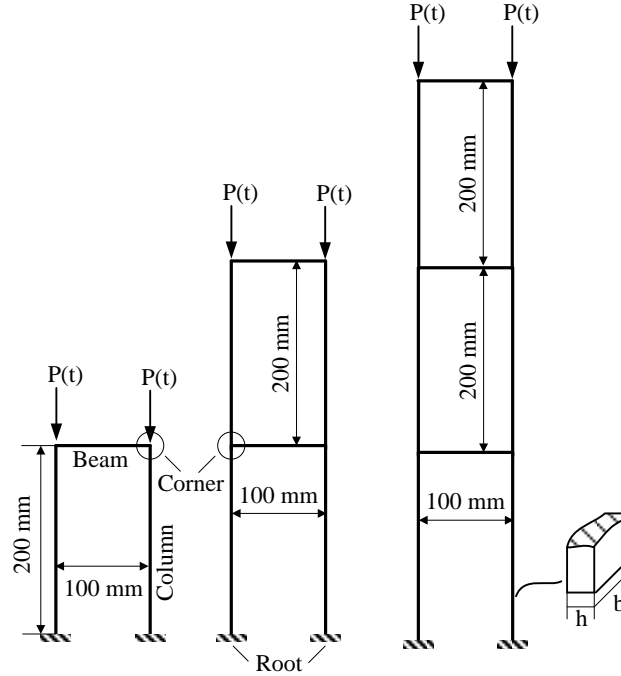


Fig. 3 Frame structures: one-storey frame, two-storey frame and three storey frame

$$\left[[K_e] - P_{cr} [K_{ge}] \right] \{\bar{q}\} = 0 \quad (22)$$

iii. Dynamic stability when all terms are present.

$$\left[[K_e] - \left(\alpha \mp \frac{1}{2} \beta \right) P_{cr} [K_{ge}] - \frac{\Omega^2}{4} [M_e] \right] \{\bar{q}\} = 0 \quad (23)$$

4. Results and discussion

4.1 Results comparison

In this study, the cracked multi-storey frames constituted by columns and beams, having rectangular cross-sections are used of which the dimensions and material properties are given in Table 1. For uncracked and cracked one-storey frames, a comparison is made between the critical buckling loads of cracked frame obtained using the present model with the results obtained from the ANSYS software. ANSYS modeling is built according to Phan (2010) which uses KSCON a concentration of key-points in circles around the crack tip. One-storey frame structure is divided into three meshed areas depending on the distance from the crack tip. First area surrounding the crack tip is meshed with $2.5e-4$ m element size. The meshing size of second area is $3e-4$ m where the rest of structure is meshed with $5e-04$ m. These patterns are applied by using face sizing for the first two areas and normal meshing for the third area which allow to calculate accurate results for the effect of crack and save memory (Ozturk *et al.* 2016). As seen from Table 2, the maximum

Table 1 Properties of the frame structure

Properties		Quantity
Modulus of elasticity, E		200 GPa
Mass density, ρ		7900 kg/m ³
Cross-section	h	5 mm
	b	20 mm
Column length		200 mm
Beam length		100 mm

Table 2 Comparison between present work and ANSYS results for the one-storey frame.

	Critical Buckling Load (N)		ERROR%
	Present Work	ANSYS	
Without crack	8747.8	8772.8	0.285%
With crack ratio ($a/h=0.5$) and crack location (1 st node)	8557.4	8503.9	0.629%

error is 0.629% and the comparison shows that very good agreement between the results is obtained. Moreover, the comparison between the natural frequencies of cracked frames obtained using the present model with the results obtained from the ANSYS software and the effect of crack on the natural frequencies have been studied by the authors (Ibrahim *et al.*, 2013); therefore, the results dealing with the natural frequencies are not given in this study.

4.2 Static stability analysis

The effects of crack location and crack ratio (a/h) or crack depth on the critical buckling load of frame structures having one, two and three storey frames are shown in Figs. 4-6. When the crack depth increases, the variations of the critical buckling load become explicit. While the crack location changes for the $a/h=0.5$, the variation in the critical buckling load of one-storey frame structure is centered symmetrically around the 15th node of the FE as seen in Fig. 4. The maximum decreases in the critical buckling load occur when the crack is at the fixed points (roots of the frame) for the one-storey frame structure.

As seen in Figs. 5 and 6, the variations in the critical buckling load of two and three-storey frame structures are not centered symmetrically. When the crack location is at the 11th and 20th nodes (corners at the beginning of the second storey), the 41th and 50th nodes (corners at the beginning of the third storey), respectively for two and three storey frame structures, the maximum decreases in the critical buckling load occur.

The maximum decreases in the critical buckling load occur when the crack is at the 1th and 30th nodes (roots of the first storey), the 11th and 20th nodes (root of the second storey), the 41th and 50th nodes (roots of the third storey) respectively for one, two and three-storey frame structures. These are about 2.17%, 2.844% and 2.597% with respect to the critical buckling load of the frame with the crack as listed in Table 3, which indicates crack location, the critical buckling loads of cracked structure, percentage of decreases and the critical buckling load without crack. In addition, when the results obtained from the static stability analysis (buckling) of multi-storey frames are evaluated, it is observed that generally the critical buckling load decreases when the crack is

located either at the roots or at the corner of the frames for multi-storey frames, as shown in Figs. 4, 5 and 6.

4.3 Dynamic stability analysis

In this study, the first instability region is studied, since this is the most dangerous region.

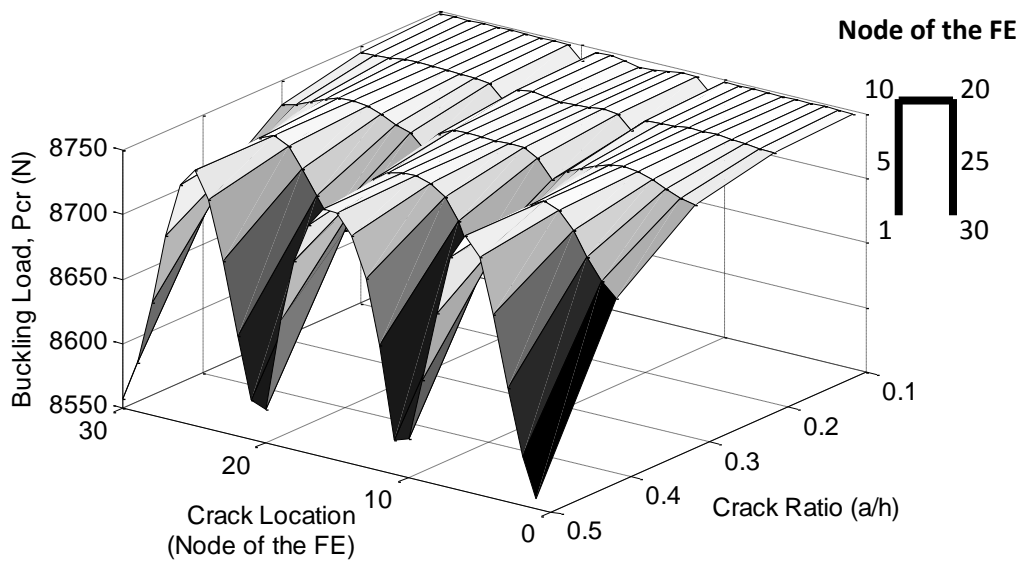


Fig. 4 The critical buckling load on the one-storey frame structure

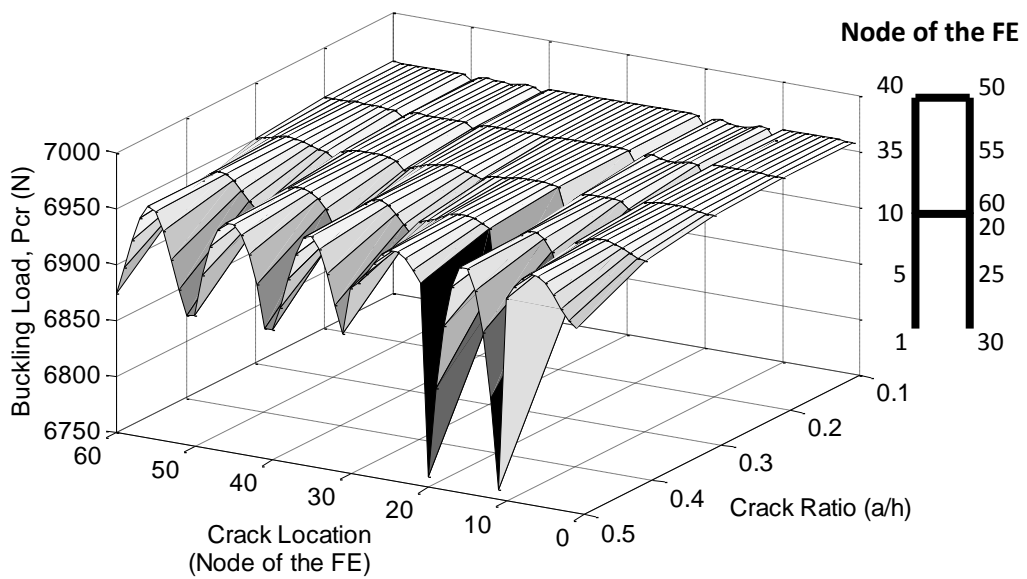


Fig. 5 The critical buckling load on the two-storey frame structure

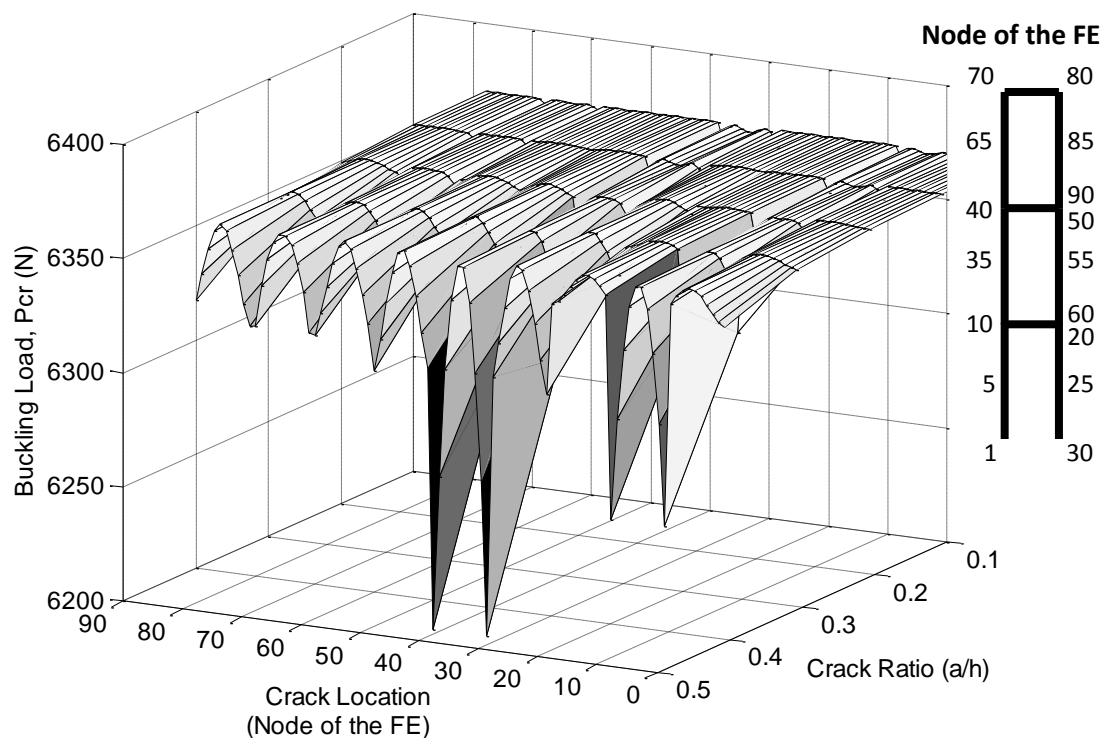


Fig. 6 The critical buckling load on the three-storey frame structure

Table 3 Percentage decrease in the critical buckling load at the maximum affected location of crack with crack ratio ($a/h=0.5$)

	One-storey frame	Two -storey frame	Three -storey frame
Maximum effected crack location	1 st , 30 th	11 st , 20 th	41 th , 50 th
Critical buckling load with crack (N)	8557.4	6759.3	6187.1
Critical buckling load without crack (N)	8747.9	6957.2	6352.1
Percentage of decrease in the critical buckling load	2.17%	2.844%	2.597%

Therefore it has the greatest practical importance (Bolotin 1967). Figures from 7 to 12 show the effects of dynamic load parameter (β), static load parameter (α) and the crack location on the dynamic instability region of multi-storey frame structures, as 3D plots. The crack depth ratio (a/h) is taken as 0.5, because the effect of this value on the unstable region is larger. It can easily be noticed that the unstable region widens as the dynamic load parameter β increases, as seen from Figs. 7 to 12. The width of unstable region of frames with a different number of storeys is arranged as one-storey, two-storey and three-storey frames, respectively. Otherwise, the initial exciting frequency ($\beta=0$) of the three-storey frame is closer to the origin than the others. It can be said that when the number of storeys increases, the initial exciting frequency of the unstable region is shifted down in parallel along the frequency axis. Thus, the risk of entering the unstable region may be increased. The regions of dynamic instability are shifted down, as the static load parameter

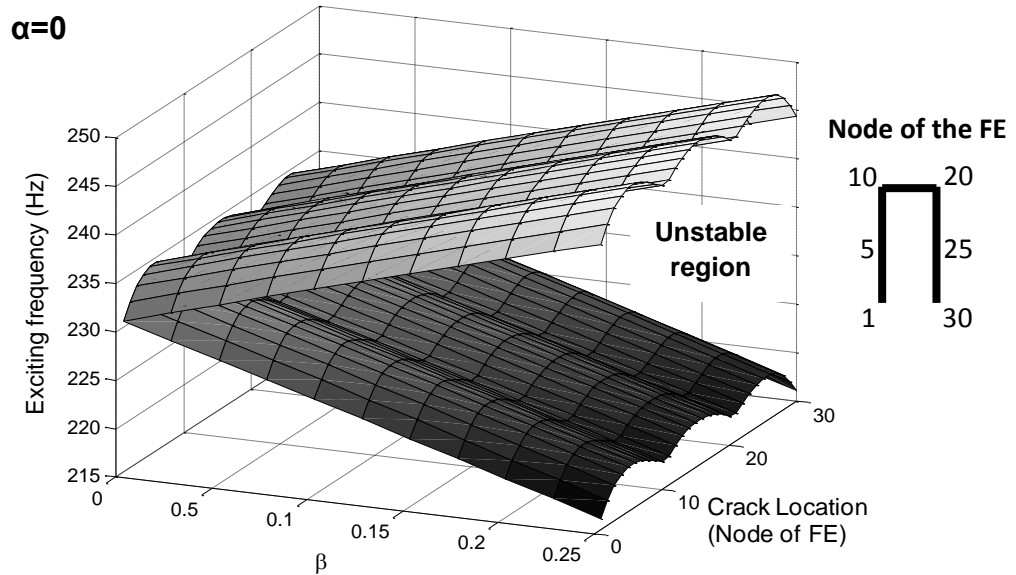


Fig. 7 The first dynamic instability region of one-storey frame structure for $\alpha=0$

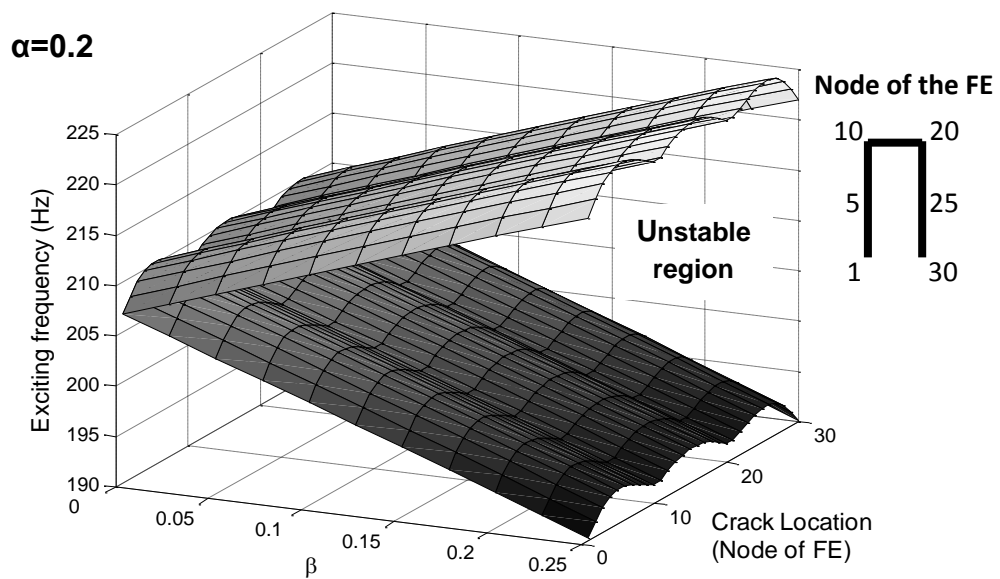


Fig. 8 The first dynamic instability region of one-storey frame structure for $\alpha=0.2$

increases as seen from Figs. 8, 10 and 12. In this case, the frame under periodic loading becomes unstable at a small exciting frequency and small dynamic load parameter. Similar to the buckling analysis, the unstable region of all frames shows a variation according to the crack location. When the crack location is at the roots or corners of frames, the first dynamic unstable region is shifted down. However, the effect of the crack location on the dynamic unstable region is greater at 1st and

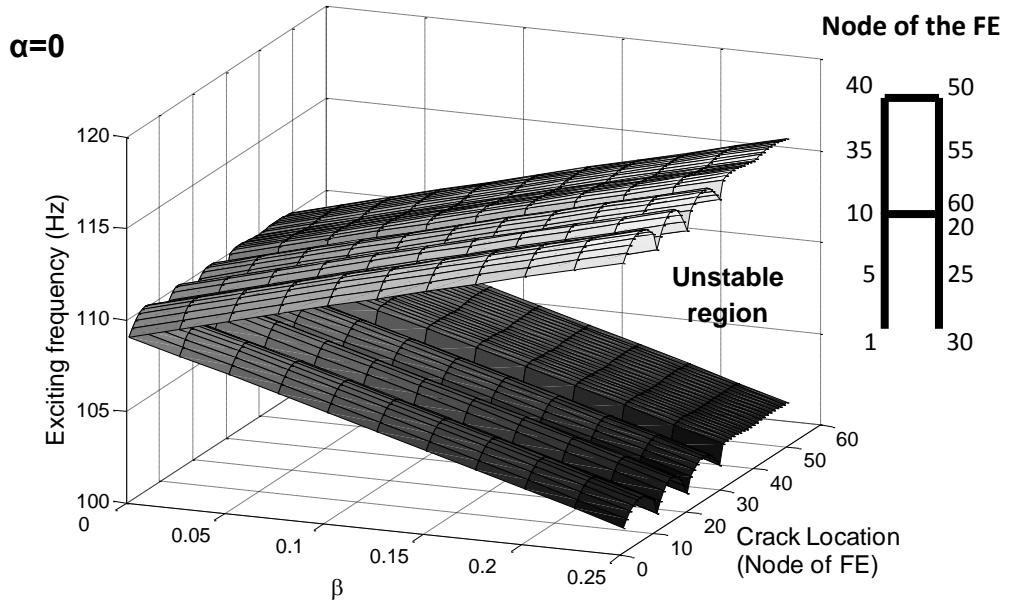


Fig. 9 The first dynamic instability region of two-storey frame structure for $\alpha=0$

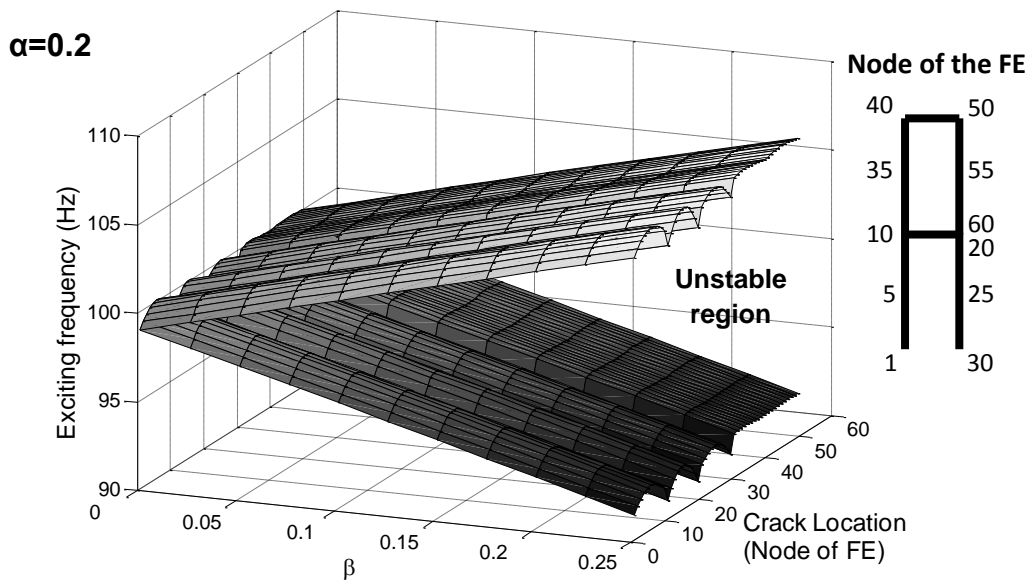


Fig. 10 The first dynamic instability region of two-storey frame structure for $\alpha=0.2$

30th nodes.

Figures from 13 to 15 present the effect of the static load parameters ($\alpha=0$ and $\alpha=0.2$) and dynamic load parameters ($\beta=0-0.25$) on the unstable regions at the most effected location of crack for crack ratio, $a/h=0.5$. As seen in Figs. 13-15, the effect of the static and dynamic load parameters on the unstable regions of the cracked frame structure is similar to the results given in

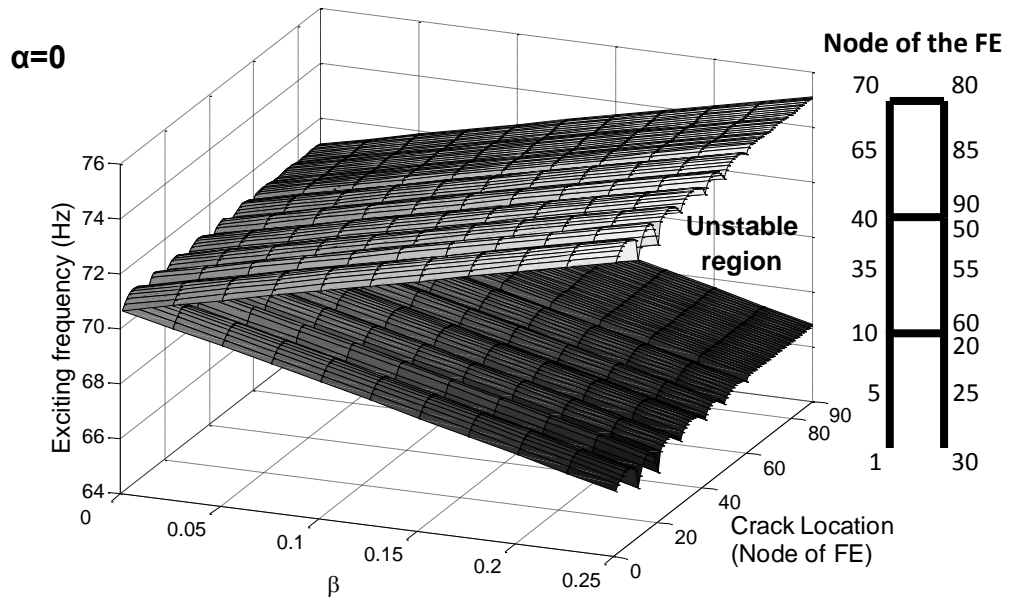


Fig. 11 The first dynamic instability region of three-storey frame structure for $\alpha=0$

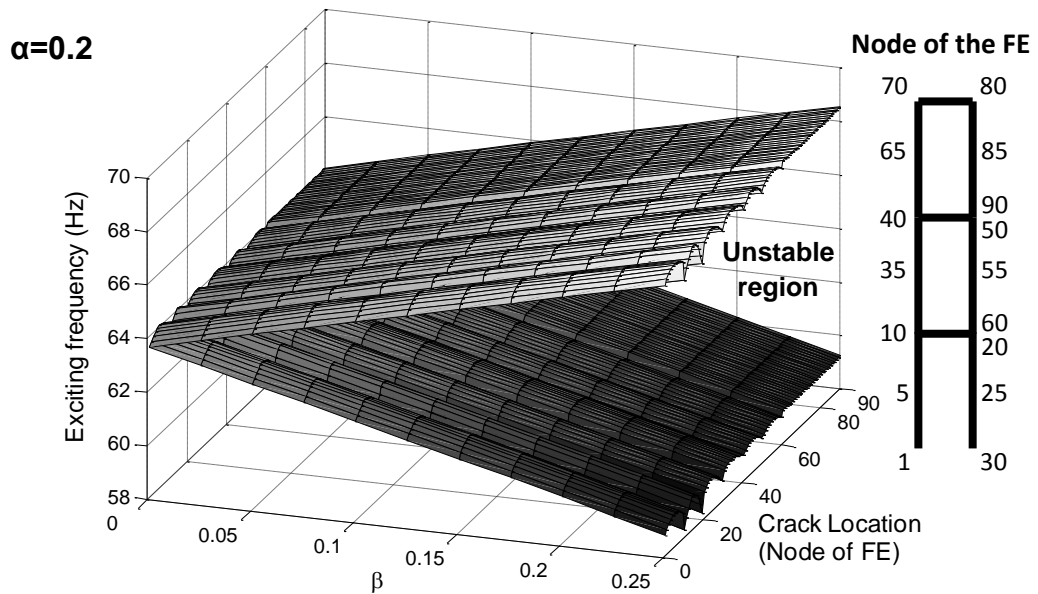


Fig. 12 The first dynamic instability region of three-storey frame structure for $\alpha=0.2$

Figs. 7-12. When the static load parameter is zero, the exciting frequency constructing the lower border of unstable region reaches zero value at which dynamic load parameter (β) corresponds to the value of 2. On the other hand, when the static load factor increases ($\alpha=0.2$), the regions of dynamic instability are shifted down and the exciting frequency constructing the lower border of

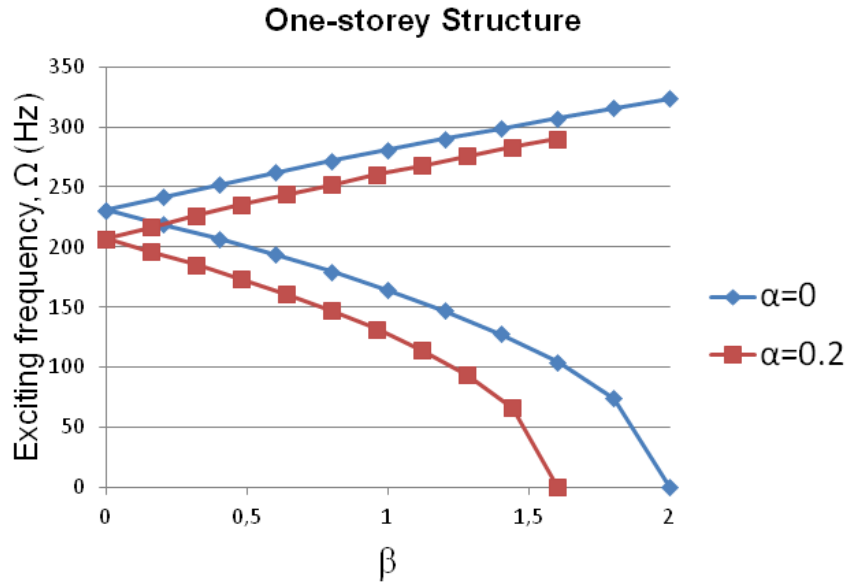


Fig. 13 The first dynamic instability regions of one-storey frame structure at the maximum affected location of crack

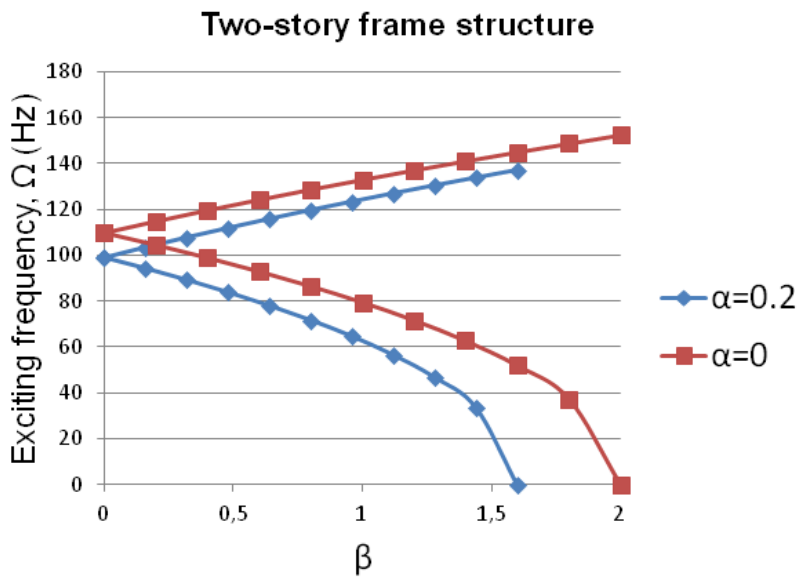


Fig. 14 The first dynamic instability regions of two-storey frame structure at the maximum affected location of crack

the unstable region reaches zero value at which the dynamic load parameter (β) corresponds to the value of 1.6.

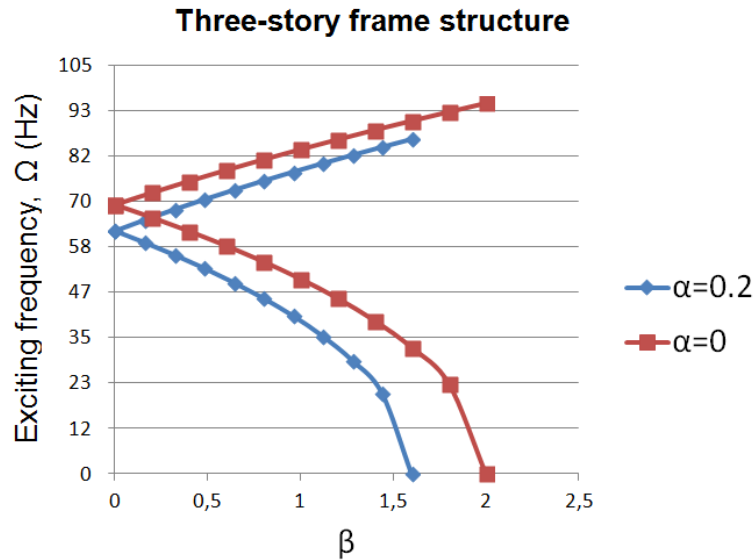


Fig. 15 The first dynamic instability regions of three-storey frame structure at the maximum affected location of crack

5. Conclusions

In this study, a cracked beam element has been used to investigate the effects of crack depth (a/h) and crack location on the in-plane static and dynamic stability of cracked multi-storey frame structures and the following conclusions are drawn:

- The crack element developed in the study is useful for the multi-storey frames. This element allows to use less finite elements according to Packet software (such as ANSYS, etc.) and thus, the eigenvalue problem solutions will be faster.
- The storey frames are set in descending order with respect to their buckling loads: one-storey, two- storey and three- storey frames.
- The reduction of the critical buckling load depends on the crack depth and crack location.
- The crack does not affect the critical buckling load of the multi-storey framed structure when it is located at the particular points of the column and the beam lengths, since the stresses in these points are smaller in comparison than the other points.
- Higher drops in the in-plane buckling load (static stability) and the exciting frequency (dynamic stability) are observed when the crack is located near the roots or corners of the frames.
- The widths of unstable regions of multi-storey frames with respect to a different number of storey frames are set in descending order as one- storey, two- storey and three- storey frames.
- Although the effect of the crack ratio (or crack depth) on the width and position of the unstable region is little, an increase in the static load parameter has strong influence on the position of the unstable region.

References

- Bolotin, V.V. (1964), *The Dynamic Stability of Elastic Systems*, Holden-Day series in mathematical Physics, Holden-Day, San Francisco.
- Briseghella, L., Majorana, C.E. and Pellegrino, C. (1998), "Dynamic stability of elastic structures: a finite element approach", *Comput. Struct.*, **69**(1), 11-25.
- Caddemi, S. and Caliò, I. (2013), "The exact stability stiffness matrix for the analysis of multi-cracked frame structures", *Comput. Struct.*, **125**, 137-144.
- Choi, D.H. and Yoo, H. (2009), "Iterative system buckling analysis, considering a fictitious axial force to determine effective length factors for multi-story frames", *Eng. Struct.*, **31**(2), 560-570.
- Girgin, Z.C. and Girgin, K. (2006), "A numerical method for static and free-vibration analysis of non-uniform Timoshenko beam-columns", *Can. J. Civil Eng.*, **33**(3), 278-293.
- Ibrahim, A.M., Ozturk, H. and Sabuncu, M. (2013), "Vibration analysis of cracked frame structures", *Struct. Eng. Mech.*, **45**(1), 33-52.
- Karaagac, C., Ozturk, H. and Sabuncu, M. (2009), "Free vibration and lateral buckling of a cantilever slender beam with an edge crack: Experimental and numerical studies", *J. Sound Vib.*, **326**(1-2), 235-250.
- Labib, A., Kennedy, D. and Featherston, C. (2014), "Free vibration analysis of beams and frames with multiple cracks for damage detection", *J. Sound Vib.*, **333**(20), 4991-5003.
- Mohammed, G.A. (2001), "Experimental and numerical analyses of multi-storey cracked frames with loss of support", *Structural Engineering, Mechanics and Computation*, Ed. A. Zingoni, Elsevier Science Ltd.
- Ozmen, G. and Girgin, K. (2005), "Buckling lengths of unbraced multi-storey frame columns", *Struct. Eng. Mech.*, **19**(1), 55-71.
- Ozturk H., Yashar, A. and Sabuncu, M. (2016), "Dynamic stability of cracked multi-bay frame structures", *Mech. Adv. Mater. Struc.*, **23**(6), 715-726.
- Phan, A.V. (2010), "ANSYS TUTORIAL-2-D Fracture Analysis ANSYS Release 7.0", University of South Alabama
- Sakar, G., Ozturk, H. and Sabuncu, M. (2012), "Dynamic stability of multi-span frames subjected to periodic loading", *J. Constr. Steel Res.*, **70**, 65-70.
- Xu, L. and Liu, Y. (2002), "Story stability of semi-braced steel frames", *J. Constr. Steel Res.*, **58**(4), 467-491.
- Xu, L. and Wang, X.H. (2007), "Stability of multi-storey unbraced steel frames subjected to variable loading", *J. Constr. Steel Res.*, **63**(11), 1506-1514.
- Xu, L. and Zhuang, Y. (2014), "Storey stability of unbraced steel frames subjected to non-uniform elevated temperature distribution", *Eng. Struct.*, **62-63**, 164-173.
- Zheng, D.Y. and Kessissoglou, N.J. (2004), "Free vibration analysis of a cracked beam by finite element method", *J. Sound Vib.*, **273**(3), 457-475.

Appendix

$$F1(s) = \sqrt{\frac{\tan\left(\frac{\pi s}{2}\right) 0.752 + 2.02s + 0.37\left(1 - \sin\left(\frac{\pi s}{2}\right)\right)^3}{\left(\frac{\pi s}{2}\right) \cos\left(\frac{\pi s}{2}\right)}} \quad (\text{A.1})$$

$$F2(s) = \sqrt{\frac{\tan\left(\frac{\pi s}{2}\right) 0.923 + 0.199\left(1 - \sin\left(\frac{\pi s}{2}\right)\right)^4}{\left(\frac{\pi s}{2}\right) \cos\left(\frac{\pi s}{2}\right)}} \quad (\text{A.2})$$

$$F3(s) = \frac{1.122 - 0.561s + 0.085s^2 + 0.18s^3}{\sqrt{1-s}} \quad (\text{A.3})$$